

Thermally activated magnetization reversal in nanometer-size iron particles

S. Wirth,^{1,2} A. Anane,¹ and S. von Molnár¹

¹MARTECH, Florida State University, Tallahassee, Florida 32306-4351

²Max Planck Institute for Chemical Physics of Solids, 01187 Dresden, Germany

(Received 24 July 2000; published 11 December 2000)

Arrays of nanometer-scale iron particles were fabricated by scanning tunneling microscopy assisted chemical vapor deposition. This allowed precise control over the particles' dimensions (diameters down to 9 nm) and their arrangement. The temperature dependence of the switching fields of these elongated particles revealed a thermally activated nucleation/propagation type of magnetization reversal even for our smallest particles. Improved high sensitivity Hall magnetometry allowed magnetic viscosity measurements which confirmed an activation volume much smaller than the particle size.

DOI: 10.1103/PhysRevB.63.012402

PACS number(s): 75.50.Tt, 07.79.Cz, 75.50.Bb, 75.60.-d

Nanometer-scale magnetic particles attract much interest since they can be used for testing basic concepts of ferromagnetism and, possibly, for applications in high density magnetic storage. These goals, however, call for extremely small particles which are well shaped and arranged and, hence, ever more demanding fabrication procedures. They include electron and ion beam and interference lithography, electrodeposition, as well as scanning tunneling microscopy (STM) assisted methods. The particle sizes often approach or may even be smaller than the superparamagnetic limit which restricts their applicability for data storage.¹ A second limitation for ever higher storage densities arises from particle interactions: The closer the particles are packed the stronger their interactions. This effect becomes even more important for particles small enough such that thermal activation reduces their individual coercivities. Moreover, it is a challenge to measure the magnetic properties of extremely small volumes. dc micro-SQUIDS,^{2,3} magnetic force microscopy (MFM), and Hall magnetometry⁴ have been successfully applied.

Here we report on the magnetic properties of well-shaped iron particles of nanometer size (diameter 9–20 nm, height of 50–250 nm for the different arrays) which were grown as arrays with varying particle number and arrangement and onto different (nonmagnetic and magnetic) substrates. Reversible and irreversible magnetization processes were analyzed from hysteresis and magnetic viscosity measurements using Hall gradiometry^{5,6} up to 100 K. To broaden the covered temperature range, MFM measurements were performed at room temperature. This has permitted detailed studies of thermally activated magnetization reversal which has been analyzed using a phenomenological description.

Arrays of iron particles were fabricated by a combination of chemical vapor deposition (CVD) and STM.^{7,8} An advantage of this method is that the particles' height and their location with respect to each other and to any feature on the sample surface can easily be controlled by steering the STM tip. At present, particles with diameters ranging from 9–20 nm and heights between 50–250 nm have been grown in square and triangular arrangements onto gold and permalloy films. The quoted diameters are those of the magnetic cores of the particles (consisting of bcc iron as revealed by TEM⁷) which were surrounded by a carbon coating. The latter re-

duced oxidation of the samples in air.⁹ For arrays grown onto gold, interaction effects between the particles could be neglected (interaction field ≤ 1 mT). Growth onto permalloy led to enhanced interactions.¹⁰ It should be noted that the precise arrangement and perfect alignment of the particles along with a controlled interaction between them presents a major advantage for detailed analysis of their magnetic properties.

Hall measurements were performed for temperatures from 5 to 100 K and in fields up to 1.5 T applied at various angles ϑ with respect to the particles' long axes. Optimal sensitivity was achieved if the array to be measured and the underlying Hall cross (onto which the array was directly grown) matched in size.¹¹ Hence, the smaller the array intended to be measured the smaller a Hall cross had to be fabricated beforehand. The 4×4 particle array shown in Fig. 1 was grown onto a Hall cross of $1 \times 1 \mu\text{m}^2$ and slightly off center. We emphasize that STM-assisted growth appears to be perfectly suitable for growing the particles at a predetermined location. The peculiar arrangement of the particles in Fig. 1 (right) was caused by a relaxation of the STM-piezo tube.

At room temperature, magnetization switching was observed by taking MFM images *after* applying field pulses of up to 0.3 T perpendicular to the image plane. This procedure

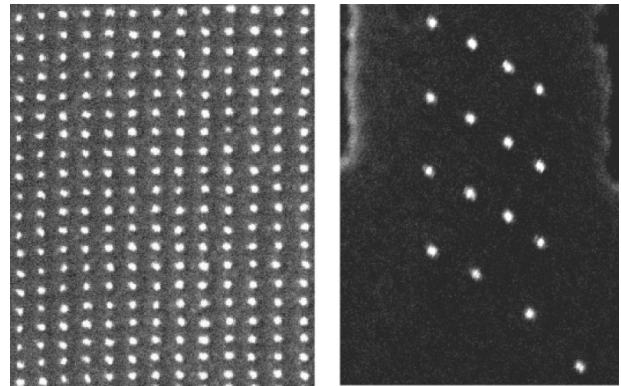


FIG. 1. SEM images of two arrays. The left one shows part of an array of 600 particles (images size $2.8 \times 3.5 \mu\text{m}^2$) whereas a small array grown onto a Hall cross of $1 \times 1 \mu\text{m}^2$ is presented on the right (images size $1.1 \times 1.5 \mu\text{m}^2$, one current leg can be recognized on the top).

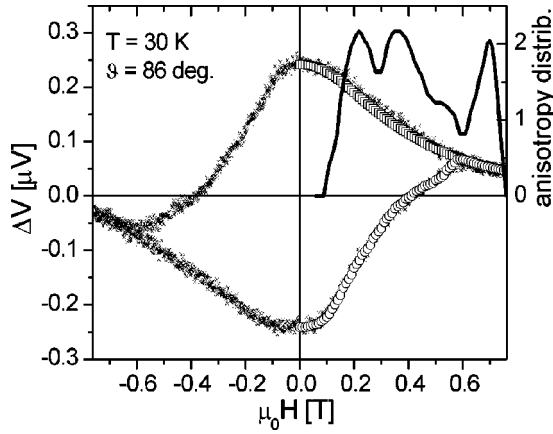


FIG. 2. Hysteresis curve (\times) of a particle array (mean diameter 17 nm) for field applied 86° with respect to the particles' EMD. Fits account for reversible (first and third quadrant, \square) and reversible and irreversible (second and fourth quadrant, \circ) magnetization processes. From the "difference," the irreversible contributions, i.e., the anisotropy distribution, can be evaluated (line, right axis).

was reliable as long as the mean particle switching field H_{sw} was higher than the field caused by the MFM-tip (~ 40 mT, Ref. 12). For smaller H_{sw} the particle magnetization did depend on the direction of the tip magnetization and H_{sw} could only be estimated (Fig. 3, 10 nm particles). Note that MFM did not show any remanent magnetization of the 9 nm particles.

For our elongated particles with aspect ratios up to 20:1, a shape anisotropy constant $K_S = (N_\perp - N_\parallel)J_S^2/2\mu_0$ (N_\parallel and N_\perp are the demagnetization factors, J_S is the spontaneous polarization) as high as 750 kJm^{-3} could be expected. Since magnetocrystalline anisotropy in iron is much smaller, the particles' long axis formed an easy magnetization direction (EMD). For fields applied parallel to the EMD switching of the particle magnetization was observed whereas for fields exactly perpendicular to the EMD only reversible rotation was expected. An indication for the latter was given by field demagnetization of an array in a perpendicular field: After reducing the field from a sufficiently high value the particles' magnetization could rotate toward either direction of the EMD with equal probability leading to zero total array magnetization.⁶ For any arbitrary field angle ϑ both mechanisms contributed to the total magnetization.

Reversible magnetization processes can be analyzed by minimizing the free energy density

$$f = K_S \sin^2 \varphi - J_S H \cos(\vartheta - \varphi) \quad (1)$$

with φ being the equilibrium orientation of the particle magnetization with respect to the EMD. Note that this analysis can even be applied for multigrain or interacting particles.¹⁴ For the particles in a given arrays, ϑ was taken to be constant whereas a distribution of K_S was assumed in calculating f and, consequently, the total magnetization of the array. In contrast, irreversible processes can only be analyzed if the exact magnetization reversal *mode* is known. One example would be uniform magnetization reversal in extremely small particles.^{3,15} However, the switching field $H_{sw}(\vartheta)$ ap-

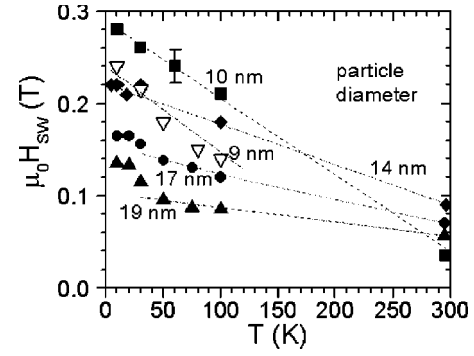


FIG. 3. Temperature dependence of the mean value of the switching field for arrays of particles of different diameter. Low temperature ($T \leq 100$ K) values were obtained by Hall magnetometry, room temperature values by MFM.

proaches the value predicted for coherent magnetization reversal in noninteracting small (single domain) particles independent of the reversal mode if $\vartheta \rightarrow 90^\circ$

$$H_{sw} = H_A (\sin^{2/3} \vartheta + \cos^{2/3} \vartheta)^{-3/2} \quad (2)$$

with $H_A = 2K_S/J_S$. Hence, also irreversible processes can be evaluated if ϑ is close to 90° (but not $\vartheta = 90^\circ$, because of field-demagnetizing effects as discussed above). With this, hysteresis curves taken in the first/third and second/fourth quadrant could be fitted simultaneously (Fig. 2, $\vartheta = 86^\circ$). In the former only reversible and in the latter both reversible and irreversible processes were taken into account. The relative number of particles switching within a certain field interval was determined from the additional change in magnetization in the fourth quadrant compared to the first, taking into account particle magnetizations already reversed at lower fields and the equilibrium orientation for non-switched and switched magnetizations from Eq. (1). The result for the irreversible processes is then related to the anisotropy (K_S) distribution of the particles (Fig. 2, line).

The average particle switching fields (which, for $\vartheta = 0^\circ$, equals the coercive field H_c) for different temperatures are presented in Fig. 3. In order to neglect thermal activation "zero" temperature values $\mu_0 H_{sw}^0$ were estimated and listed in Table I. These numbers are much smaller than predicted for uniform magnetization reversal, and hence our particle magnetizations reversed by inhomogeneous modes. The unusually broad distribution of K_S found for the 17 nm particles (Fig. 2) does not influence this conclusion. One likely

TABLE I. Estimated "zero" temperature switching fields H_{sw} , the distribution $\Delta H_{sw} = H_{sw}^{\max} - H_{sw}^{\min}$ of switching fields at 30 K and mean critical volumes \hat{v}_{cr} derived from $H_{sw}(T)$ for the different particle diameters investigated.

Mean diameter d [nm]	9	10	14	17	19
$\mu_0 H_{sw}^0$ [mT]	242	288	223	165	135
$\mu_0 \Delta H_{sw}$ (30 K) [mT]	~ 90	80	80	140	120
\hat{v}_{cr} [nm ³]	210	260	470	720	1200
\hat{v}_{cr}/d^2 [nm]	2.6	2.6	2.4	2.5	3.3

mode is curling.¹⁶ Here, a d^{-2} dependence of H_{sw}^0 is expected¹³: $\mu_0 H_{sw}^0 = 2.16 J_S \lambda_{ex}^2 d^{-2}$ where $\lambda_{ex} = \sqrt{\mu_0 A / J_S}$ the exchange length and A is the exchange constant. We found such a dependence only for the larger particles, $d \geq 14$ nm (cf. Table I) and estimated $\lambda_{ex} = 3.1$ nm and $A \sim 36$ pJm⁻¹ in agreement with Ref. 17. For the smaller particles, the reversal mode could be of buckling type.¹³ The 9 nm particles may have consisted of more than one grain per particle leading to reduced H_{sw} .

The rapid decrease of $H_{sw}(T)$ (Fig. 3) can obviously not be explained by changing material properties only. Hence, thermal fluctuations influencing the magnetization reversal process must be taken into consideration.^{18,19} A phenomenological model was previously introduced⁸ that did *not* invoke the common assumption of uniform magnetization rotation for calculating the energy barrier. This model rather relied on the concept of a critical volume v_{cr} within which a nucleus of reversed magnetization was formed by thermal activation. The thermal energy must overcome the energy needed for the formation of a wall (that separated the nucleus from the remainder of the particle) and magnetostatic energy²⁰

$$k_B T \ln(t/\tau_0) = \alpha \gamma \frac{\pi d^2}{4} - H J_S \int_{v_{min}}^{v_{max}} dv_{cr}, \quad (3)$$

where γ referred to the wall energy density, α accounted for the number of domain walls formed as well as for shape inhomogeneities of the particles and τ_0 was the attempt time ($\sim 10^{-9}$ s). The thermal energy was estimated within the *critical volume approach*²¹ considering the sharp peak of its distribution. For our small particles, the nucleus was assumed to cover the particles' cross section. The mean value \hat{v}_{cr} of the critical volume is then related to the measured switching field

$$H_{sw} = \frac{\alpha \gamma \pi d^2}{4 \hat{v}_{cr} J_S} - \frac{25 k_B T}{\hat{v}_{cr} J_S}. \quad (4)$$

Temperature and field independent \hat{v}_{cr} can be assumed due to weak temperature dependences of the material properties and independent experimental findings.^{22,23} The applicability of this model for the 14 nm particles was supported by comparing H_{sw} measured for different angles ϑ to the predicted values.⁶ Moreover, the concept of this model can favorably be compared to analytic calculations²⁴ and numerical simulations.²⁵

Fitting the experimental values $H_{sw}(T)$ to Eq. (4) results in almost straight lines shown in Fig. 3 [the temperature dependence of $J_S(T)$ was taken into account]. The obtained values of \hat{v}_{cr} are listed in Table I. Note that \hat{v}_{cr} is mainly determined by the second term in Eq. (4). The first term is much more difficult to evaluate, especially since γ can be estimated only roughly. Most remarkably, Brown¹⁹ gave the upper volume limit of a superparamagnetic iron sphere to be 270 nm³, in excellent agreement with our findings: At room temperature, the 10 nm particles were very close to the superparamagnetic limit whereas the 9 nm particles appeared to be below this limit. This suggests the interpretation that our

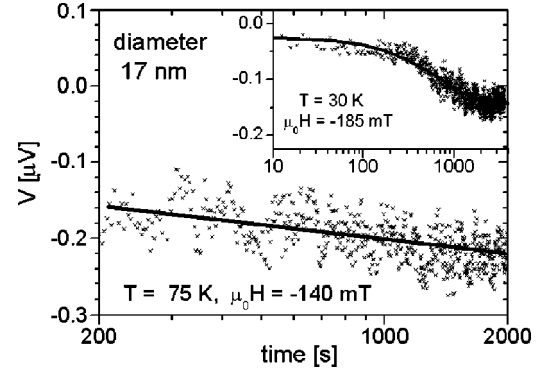


FIG. 4. Measured time dependence of the total polarization of a particle array. The line presents the result of a fit to a logarithmic law. For an extended time range (inset, same array under different conditions) probabilities for thermally activated reversal have to be considered.

\hat{v}_{cr} is the minimum volume required to initiate magnetization reversal in the particles. The necessary energy for switching the 9 nm particles was provided solely thermally at room temperature and the longitudinal relaxation time was estimated²⁶ to be in the order of 10^{-3} s. This time could, however, be somewhat reduced since the magnetization reversal may take place via a complex path in configuration space.^{27,28} The bigger the particles the larger \hat{v}_{cr} . For the biggest particles (17 and 19 nm) and with constant times t for all $H_{sw}(T)$ measurements, the thermal energy at low temperature was not sufficient to provide nuclei with sufficient probability and induce the nucleation/propagation process. This may have caused the increased values of $H_{sw}(T)$ for these particles (Fig. 3).

As an independent check of our results magnetic viscosity experiments were attempted. Here, the array was completely magnetized in one direction, $\vartheta = 0^\circ$. Subsequently the field was reversed to a value close to H_{sw} and held constant while the time dependence of the array's magnetization was recorded. Special care was taken to detect any drift in the experimental setup. A result of such a measurement is shown in Fig. 4 for 17 nm particles at 75 K. As expected from Eq. (3) a logarithmic dependence of total array magnetization on time was found for an *intermediate* time range: $J(t) = J(0) - S \ln(t/t')$ with S being the magnetic viscosity. This may be understood¹⁸ by a sufficiently broad spectrum (Fig. 2) of energy barriers of the particles switching (about 14 in the time range shown, the magnetization reversal of individual particles could not be resolved). Using different conditions (inset in Fig. 4, see also Ref. 28) the onset and trail off of thermally activated magnetization reversal was observed. This was to be expected by evaluation of the integral Eq. (3). The line was calculated from an exponential law for the switching probabilities. The comparison of field driven and thermally activated magnetization reversal (assuming the same barriers have to be overcome) yielded an activation volume

$$v_A = \frac{k_B T}{J_S} \frac{\mu_0 \chi_{irr}}{S} \quad (5)$$

which gave the typical volume involved in a single activation process.²⁹ The irreversible susceptibility χ_{irr} was taken from magnetization curves $\vartheta=0$. For the conditions of Fig. 4, $v_A \approx 250 \text{ nm}^3$. Similar results were obtained in the temperature range 10–60 K. Considering the different concepts involved, v_A and \hat{v}_{cr} were found to be in reasonable agreement. Note that our results for v_A are somewhat smaller if compared to Ref. 22, 23 and 30. However, in contrast to those, we investigated an extremely small total magnetic volume of identical particles. Thus interparticle interactions as well as particle misalignments could be excluded to a large extent.

Recently, numerical simulations³¹ indicated that the exact shape of extremely small particles (like sharp corners) does not significantly influence their switching due to the dominance of exchange interactions. Hence, the differences in magnetization reversal for different arrays were most likely related to their different particle diameters rather than different morphologies as long as multiple grains per particle can be excluded. Although the above model described well the magnetization reversal of our very small particles (\hat{v}_{cr}/d^2 in Table I) the results for the 19 nm particles may indicate that

the critical volume for particles of larger diameter scales to a higher order than d^2 ($v_A \propto d^3$ in Ref. 22). Our assumption that v_{cr} covered the particles' cross section certainly breaks down for larger diameters. Hence, other reversal modes needed to be considered, e.g., thermal activation in conjunction with curling or other collective processes.²³ In any event, \hat{v}_{cr} and v_A were much smaller than the particle volume, indicating again that nonuniform magnetization processes dominated even on a 10 nm scale.

In conclusion, we studied the reversible and irreversible magnetization processes of iron particles with diameters ranging from 9 to 19 nm. Nonuniform magnetization reversal was found for all diameters. Thermal activation strongly reduced the particles' switching field with increasing temperature. Magnetic viscosity experiments confirmed a critical volume for thermally activated reversal as derived from a phenomenological model.

This work was supported by the Office of Naval Research under Grant No. NSF-DMR-0072395 and by the Air Force under Grant No. F49620-96-1-0026.

-
- ¹D. Weller and A. Moser, *IEEE Trans. Magn.* **35**, 4423 (1999).
²W. Wernsdorfer *et al.*, *Phys. Rev. Lett.* **78**, 1791 (1997); W. Wernsdorfer *et al.*, *ibid.* **84**, 2965 (2000).
³E. Bonet *et al.*, *Phys. Rev. Lett.* **83**, 4188 (1999).
⁴S. J. Bending, *Adv. Phys.* **48**, 449 (1999).
⁵A. D. Kent *et al.*, *J. Appl. Phys.* **76**, 6656 (1994).
⁶S. Wirth *et al.*, *J. Appl. Phys.* **85**, 5249 (1999).
⁷A. D. Kent *et al.*, *Science* **262**, 1249 (1993).
⁸S. Wirth *et al.*, *Phys. Rev. B* **57**, R14 028 (1998).
⁹Our oldest sample did not show any deterioration of its magnetic properties after almost 3 years.
¹⁰S. Wirth and S. von Molnár, *J. Appl. Phys.* **87**, 7010 (2000).
¹¹S. Wirth *et al.*, *Appl. Phys. Lett.* **76**, 3283 (2000).
¹²S. L. Tomlinson and E. W. Hill, *J. Magn. Magn. Mater.* **161**, 385 (1996).
¹³A. Aharoni, *Introduction to the Theory of Ferromagnetism* (Oxford University Press, Oxford, 1996).
¹⁴S. Wirth, *10th International Symposium Magnetic Anisotropy Coercivity in RE-TM Alloys* (Dresden, Germany, 1998), p. 139.
¹⁵E. C. Stoner and E. P. Wohlfarth, *Philos. Trans. R. Soc. London* **240**, 599 (1948).
¹⁶W. F. Brown, Jr., *Phys. Rev.* **105**, 1479 (1957); E. H. Frei, S. Shtrikman, and D. Treves, *ibid.* **106**, 446 (1957).
¹⁷M. R. Scheinfein *et al.*, *Phys. Rev. B* **43**, 3395 (1991).
¹⁸L. Néel, *Ann. Geophys. (C.N.R.S.)* **5**, 99 (1949).
¹⁹W. F. Brown, Jr., *Phys. Rev.* **130**, 1677 (1963).
²⁰D. Givord *et al.*, *IEEE Trans. Magn.* **24**, 1921 (1988).
²¹R. W. Chantrell *et al.*, *Phys. Status Solidi A* **97**, 213 (1986).
²²F. Li, R. M. Metzger, and W. D. Doyle, *IEEE Trans. Magn.* **33**, 3715 (1997).
²³F. Wacquant *et al.*, *IEEE Trans. Magn.* **35**, 3484 (1999).
²⁴H.-B. Braun, *Phys. Rev. Lett.* **71**, 3557 (1993).
²⁵E. D. Boerner and H. N. Bertram, *IEEE Trans. Magn.* **33**, 3052 (1997); G. Brown, M. A. Novotny, and P. A. Rikvold, *J. Appl. Phys.* **87**, 4792 (2000).
²⁶W. T. Coffey *et al.*, *J. Magn. Magn. Mater.* **131**, L301 (1994).
²⁷R. Arias and H. N. Bertram, *J. Magn. Magn. Mater.* **171**, 209 (1997).
²⁸M. Lederman, S. Schultz, and M. Ozaki, *Phys. Rev. Lett.* **73**, 1986 (1994).
²⁹E. P. Wohlfarth, *J. Phys. F: Met. Phys.* **14**, L155 (1984).
³⁰S. M. Stinnett and W. D. Doyle, *IEEE Trans. Magn.* **34**, 1681 (1998).
³¹W. Rave *et al.*, *J. Magn. Magn. Mater.* **183**, 329 (1998).